

AD-A221 204

DTIC FILE COPY

②

DOCUMENTATION PAGE

Form Approved
OMB No. 0704-0188

1a. REPORT SECURITY CLASSIFICATION Unclassified			1b. RESTRICTIVE MARKINGS		
2a. SECURITY CLASSIFICATION AUTHORITY			3. DISTRIBUTION/AVAILABILITY OF REPORT DISTRIBUTION STATEMENT A Approved for public release; Distribution Unlimited		
2b. DECLASSIFICATION/DOWNGRADING SCHEDULE			5. MONITORING ORGANIZATION REPORT NUMBER(S)		
4. PERFORMING ORGANIZATION REPORT NUMBER(S)			7a. NAME OF MONITORING ORGANIZATION U.S. Army Medical Research and Development Command		
6a. NAME OF PERFORMING ORGANIZATION U.S. Army Medical Research Institute of Infectious Diseases		6b. OFFICE SYMBOL (if applicable) SGRD-UIS	7b. ADDRESS (City, State, and ZIP Code) Fort Detrick, Frederick, MD 21701-5012		
8a. NAME OF FUNDING/SPONSORING ORGANIZATION		8b. OFFICE SYMBOL (if applicable)	9. PROCUREMENT INSTRUMENT IDENTIFICATION NUMBER		
8c. ADDRESS (City, State, and ZIP Code)		10. SOURCE OF FUNDING NUMBERS			
		PROGRAM ELEMENT NO.	PROJECT NO.	TASK NO.	WORK UNIT ACCESSION NO.
11. TITLE (Include Security Classification) Toxicokinetics of [³ H]microcystin-LR in mice.					
12. PERSONAL AUTHOR(S) Nancy A. Robinson, Judith G. Pace, Charles F. Matson, George A. Miura and Wade B. Lawrence					
13a. TYPE OF REPORT Interim		13b. TIME COVERED FROM _____ TO _____		14. DATE OF REPORT (Year, Month, Day) 900319	
				15. PAGE COUNT 34	
16. SUPPLEMENTARY NOTATION					
17. COSATI CODES			18. SUBJECT TERMS (Continue on reverse if necessary and identify by block number)		
FIELD	GROUP	SUB-GROUP			
			toxicokinetics, microcystin, mice.		
19. ABSTRACT (Continue on reverse if necessary and identify by block number) The distribution, excretion, and metabolism of [³ H]microcystin-LR ([³ H]MCYST-LR, sublethal, iv) were measured in mice. Plasma elimination was biexponential with α - and β -phase half-lives of 0.8 and 6.9 min, respectively. The apparent volume of distribution of the β -phase was 10 ml and the bioavailability was 1036 pmol min/ml. At 60 min, liver contained $67 \pm 4\%$ of dose and the amount of hepatic radioactivity did not change through 6 days. Excretion of radiolabel, measured through 5 days, accounted for $23.7 \pm 1.7\%$ of the dose, with 9.2 ± 1 and $14.5 \pm 1.1\%$ in urine and feces, respectively. Approximately 60% of the urine and fecal radiolabel was parent. Hepatic cytosol, which contained $70 \pm 2\%$ of hepatic radiolabel, was prepared for HPLC analysis by heat denaturation, pronase treatment, and C-18 Sep Pak extraction. One hour post exposure, $35 \pm 2\%$ of the radiolabel was insoluble or C-18 Sep Pak-bound; $43 \pm 3\%$ was associated with a peak of retention time (rt) 6.6 min, and $16 \pm 3\%$ with parent. After 6 days, $8 \pm 1\%$ was C-18 Sep Pak-bound or insoluble; $5 \pm 0\%$ occurred at rt 6.6 min, $17 \pm 1\%$ with parent, and $60 \pm 2\%$ was associated with rt 8.1 min. Two other radio-active peaks, rt 4.9 and 5.6 min, appeared (See reverse side.)					
20. DISTRIBUTION/AVAILABILITY OF ABSTRACT <input type="checkbox"/> UNCLASSIFIED/UNLIMITED <input type="checkbox"/> SAME AS RPT. <input type="checkbox"/> DTIC USERS			21. ABSTRACT SECURITY CLASSIFICATION		
22a. NAME OF RESPONSIBLE INDIVIDUAL			22b. TELEPHONE (Include Area Code)		22c. OFFICE SYMBOL

Block 19 (continued)

transiently. This study is the first to describe the long-term hepatic retention of MCYST toxin and documents a putative detoxification pathway.

Toxicokinetics of [³H]Microcystin-LR in Mice

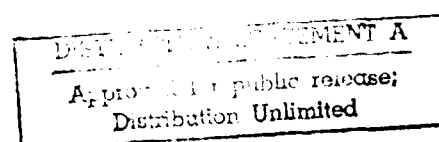
Nancy A. Robinson¹, Judith G. Pace¹, Charles F. Matson¹, George A.
Miura¹, and Wade B. Lawrence²

Pathophysiology¹ and Pathology² Divisions, United States Army
Medical Research Institute of Infectious Diseases, Fort Detrick,
Frederick, Maryland 21701-5011

Short title: MICROCYSTIN TOXICOKINETICS

Accession For	
NTIS GRA&I	<input checked="checked" type="checkbox"/>
DTIC TAB	<input type="checkbox"/>
Unannounced	<input type="checkbox"/>
Justification	<i>form 50 per</i>
By	
Distribution/	
Availability Codes	
Dist	Special
<i>A-1</i>	

Send Proofs To: Dr. Nancy A. Robinson
Pathophysiology Division
USAMRIID
Ft. Detrick
Frederick, MD 21701-5011 USA



Toxicokinetics of [^3H]Microcystin-LR in Mice. ROBINSON, N. A., PACE, J. G., MATSON, C. F., MIURA, G. A., and LAWRENCE, W. B. (1990). *Toxicol. Appl. Pharmacol.* XX, XXX-XXX. The distribution, excretion, and metabolism of [^3H]microcystin-LR ([^3H]MCYST-LR, sublethal, iv) were measured in mice. Plasma elimination was biexponential with α - and β - phase half-lives of 0.8 and 6.9 min, respectively. The apparent volume of distribution of the β -phase was 10 ml and the bioavailability was 1036 pmol min/ml. At 60 min, liver contained $67 \pm 4\%$ of dose and the amount of hepatic radioactivity did not change through 6 days. Excretion of radiolabel, measured through 6 days, accounted for $23.7 \pm 1.7\%$ of the dose, with 9.2 ± 1 and $14.5 \pm 1.1\%$ in urine and feces, respectively. Approximately 60% of the urine and fecal radiolabel was parent. Hepatic cytosol, which contained $70 \pm 2\%$ of hepatic radiolabel, was prepared for HPLC analysis by heat denaturation, pronase treatment, and C-18 Sep Pak extraction. One hour post exposure, $35 \pm 2\%$ of the radiolabel was insoluble or C-18 Sep Pak-bound; $43 \pm 3\%$ was associated with a peak of retention time (rt) 6.6 min, and $16 \pm 3\%$ with parent. After 6 days, $8 \pm 1\%$ was C-18 Sep Pak-bound or insoluble; $5 \pm 0\%$ occurred at rt 6.6 min, $17 \pm 1\%$ with parent, and $60 \pm 2\%$ was associated with rt 8.1 min. Two other radioactive peaks, rt 4.9 and 5.6 min, appeared transiently. This study is the first to describe the long-term hepatic retention of MCYST toxin and documents a putative detoxification pathway.

INTRODUCTION

Microcystin-LR (MCYST-LR), isolated from the cyanobacterium *Microcystis aeruginosa* strain PCC-7820, is one of several related cyclic hepatotoxins (Botes et al., 1985; Rinehart et al., 1988). This family of toxins has been implicated in the death of both wild and domestic animals that consumed water containing dense blooms of blue-green alga (Soll and Williams, 1985; Beasley et al., 1989; Galey et al., 1987). A consistent pathological finding after lethal exposure to toxin is blood-engorged livers with diffuse hepatic centrilobular necrosis (Konst et al., 1965; Adams et al., 1988; Jackson et al., 1984; Theiss et al., 1988; Hooser et al., 1989). The proposed cause of death is massive intrahepatic hemorrhage (Hooser et al., 1989; Theiss et al., 1988). Human fatality has not been associated with the MCYST toxins; however, a heavy bloom of *M. aeruginosa* in a reservoir at Malpus Dam, Australia, was correlated with a rise in plasma gamma-glutamyl transpeptidase in humans, suggestive of hepatic injury (Falconer et al., 1983).

While information has been published concerning the tissue distribution of MCYST toxins in rat (Falconer et al., 1986; Pace et al., 1990b) and in mouse (Robinson et al., 1989; Brooks and Codd, 1987; Runnegar et al., 1986), the toxicokinetics have not been completely described in either species. The liver, the target organ, accumulates toxin; however, the time required for maximal accumulation varies from 1 min (Brooks and Codd, 1987) to 60 min (Robinson et al., 1989) after ip administration in mice.

Additionally, metabolism and elimination of the toxin have not been measured comprehensively.

It is reasonable to propose that metabolism of MCYST-LR be necessary for its toxic effects to be expressed, based upon the following considerations: hepatic damage occurs in the centrilobular (perivenous) region, which is the location of the highest concentration of many metabolic enzymes (Jungermann and Katz, 1989); liver specificity could be explained by prerequisite hepatic metabolism for toxicity; and neonatal rats and mice are not as susceptible to the MCYST toxins (Foxall and Sasner, 1981; Stoner et al., 1989), possibly because many metabolic enzymes are regulated developmentally (Pelkonen, 1979).

We described the toxicokinetics of a sublethal, iv bolus dose of [³H]MCYST-LR in the mouse model. Reported here are the kinetics of elimination from plasma, the time course of distribution to tissues over a 60-min interval, the elimination in urine and feces through 6 days post injection, and the metabolic fate of [³H]MCYST-LR.

MATERIALS AND METHODS

Reagents. MCYST-LR (>95% purity) was supplied by W. W. Carmichael (Wright State University, Dayton OH). [^3H]MCYST-LR (Amersham Corp, Arlington Heights, IL, 40% radiochemical purity) was produced by chemical tritiation of MCYST-LR (Matsuo and Narita, 1975) and purified by reverse-phase high performance liquid chromatography (HPLC) (99% radiochemical purity, 194 mCi/mmol, Robinson et al., 1989).

Male, VAF/plus CD-1 mice [crl:CD-1(1CR)BR Charles River, Wilmington, MA], weighing 20-27 g, were maintained on a 12-hr light/dark cycle. Mice were fasted 17-20 hr before studies but allowed water *ad libitum*.

Time course of radiolabel distribution. Fasted mice were injected iv via the tail vein with 35 $\mu\text{g/kg}$ [^3H]MCYST-LR. Two min prior to obtaining blood samples, animals were anesthetized with 50 mg/kg each xylazine and ketamine by im injection (hind limb). After the brachial artery was severed, blood was collected from a skin pouch formed medial to the forelimb. Heparin (1000 U/ml, 50 μl) was added to the blood and plasma was separated by centrifugation at 700 x g for 10 min. Tissues (heart, lung, liver, gut, kidney, and spleen) were removed, weighed, minced, and digested in 2N KOH for 48 hr at 65°C. The remainder of the carcass was digested for 72 hr at 65°C. After

digestion, 100 μ l of each tissue sample was added to 200 μ l 2N HCl and 10 ml Hydrofluor (National Diagnostics, Manville, NJ). Radioactivity was measured in a Beckman 5800 liquid scintillation counter (Berkley, CA). Time points employed were 1, 3, 6, 10, 15, 20, 30, 40, and 60 min post injection.

Quantitation of radiolabel in urine, feces, and liver. Mice were housed three per Nalgene metabolic cage, (Harvard Apparatus, South Natick, MA) after iv injection of 35 μ g/kg [3 H]MCYST-LR. Urine and feces were collected at 6 and 12 hr and 1, 2, 3, 4, 5, and 6 days post exposure. Sodium fluoride (25 mg) was added to the urine samples and 100-500 μ l was analyzed for radioactivity. The calculated limit of detection in urine was 1 pmol/ml. Feces were ground in liquid nitrogen with a mortar and pestle. Weighed portions (20-30 mg) of the ground fecal material were digested in 0.2 ml of 1 N KOH for 48 hr at 65°C. The radioactivity of the entire sample was measured as described above for tissues. The calculated limit of detection in feces was 16 pmol/g. At 1, 6, and 12 hr and 1, 2, 4, and 6 days, three animals were anesthetized and their plasma collected. Livers were removed, freeze-clamped with aluminum tongs cooled with liquid nitrogen, and ground in liquid nitrogen with a mortar and pestle. Radioactivity of weighed portions (20-30 mg) of liver was measured after digestion in 2N KOH. The remainder of the carcass was digested and radioactivity measured as described above.

HPLC analysis of urine, feces and liver metabolites. HPLC was performed using a Waters system (Milford, MA) equipped with a Waters 490 multiwavelength detector. The C-18 column (Adsorbosphere HS, 4.6 x 250 mm, 5 μ m, Alltech, Deerfield, IL) was run at a flow rate of 1 ml/min of 73% 10 mM ammonium acetate, pH 6.0, and 27% acetonitrile for 15 min. Elution of radioactivity was monitored with a Flow I β -radiodetector (Radiomatic Instruments and Chemical Co., Tampa, FL), outfitted with a 5-ml cell and Flo-Scint III scintillation fluid (Radiomatic) pumped at 2 ml/min. Day-to-day variation in the retention time of standard MCYST (probably due to the contaminating components in the samples analyzed) was controlled by spiking each radioactive sample with 5 μ g of unlabeled MCYST and monitoring the elution of this internal standard by UV absorption at 238 nm. Urine (100-250 μ l) was analyzed by C-18 HPLC without prior treatment. Feces (0.1-0.5 g) were homogenized with a Polytron homogenizer (Brinkman Instrument Co, Westbury, NY) in two 4-ml portions of 50 mM ammonium acetate, pH 6.0. The supernatant fraction was obtained after centrifugation at 15,000 x g for 15 min. The fecal extract was subjected to solid-phase extraction on C-18 Sep Pak cartridges (Waters, Morristown, NJ). Radioactivity was eluted with 100% methanol. The methanol fraction was dried under N₂ at room temperature and the residue dissolved in 200 μ l of 27% acetonitrile and 73% 10 mM ammonium acetate, pH 6.0. Ground liver samples (1.5-2 g) were homogenized with a motor-driven, teflon pestle in 5 ml of 100 mM Tris-Cl, pH

7.2, and centrifuged at 10,000 x g for 10 min. The pellet was rehomogenized (3 ml buffer) and centrifuged as before. The combined supernatants were centrifuged at 100,000 x g to obtain the cytosolic fraction. The cytosol (1 ml) was heat-denatured for 30 min at 90°C after addition of an equal volume of 100 mM potassium phosphate, pH 7.5. Pronase (1 mg in 1 ml buffer, Boehringer Mannheim Biochemicals, Indianapolis, IN) was added to the heat-denatured slurry and the sample incubated for 1 hr at 37°C. The resulting solution was centrifuged to remove any particulate material and the supernatant chromatographed on C-18 Sep Pak cartridges. Radioactivity was eluted with methanol, and the sample concentrated and prepared for HPLC analysis, as described for fecal samples.

Analysis of hepatic cytosol by desalting chromatography. Econo-Pac 10DG disposable columns (Bio-Rad, Rockville Center, NY), supplied prepacked with Bio-Gel P-6 desalting gel, were used to analyze samples of hepatic cytosol (0.8 ml) isolated from livers 1 hr to 6 days post exposure to [³H]MCYST-LR. Columns were prepared with 100 mM Tris-Cl, pH 7.2, according to manufacturer's direction, except that 0.8 ml of sample rather than 3 ml was applied to the columns. Fractions (1 ml) were collected and analyzed for radioactivity by liquid scintillation.

Plasma chemistry and histology. Plasma collected from either control mice (1 hr or 6 days post injection of saline) or

toxin-treated mice (1, 6, and 12 hr and 1, 2, 4, and 6 days post injection) was analyzed on a COBAS BIO Centrifugal Analyzer (Roche Analytical Instruments, Nutley, NJ). Kits for blood urea nitrogen (BUN), lactate dehydrogenase (LDH), alanine aminotransferase (ALT), and aspartate aminotransferase (AST) were obtained from Roche. Sorbitol dehydrogenase (SDH) and Lowry total protein kits were purchased from Sigma Chemical Company (St. Louis, MO). Sections of the left lobe of liver were removed at each time point and fixed for a minimum of 24 hr in 10% neutral buffered formalin. Subsequently, tissue specimens were processed by routine paraffin-embedding techniques and sectioned at 4-6 μ m. All sections were stained with hematoxylin and eosin, and examined by light microscopy.

Data analysis. Tissue distribution data are expressed as toxin molar equivalents because individual metabolites were not determined in each tissue. The plasma concentration data were fit to a biexponential decay equation, $C = Ae^{-\alpha t} + Be^{-\beta t}$, by nonlinear regression by using Enzfitter software (Elsevier-BIOSOFT, Cambridge, UK) on a IBM personal computer AT. The half-lives ($t_{1/2}$) of the α - and β -phases were calculated by the equation

$$t_{1/2} = 0.693/k$$

where k is α or β . The maximum plasma concentration of toxin, C_0 , was calculated by using the defined plasma concentration equation at $t = 0$. Area under the curve (AUC) was calculated with the trapezoid rule. Clearance (C_l) was calculated by the

following equation:

$$C_l = \text{Dose}/\text{AUC}$$

The apparent volume of the central compartment, V_c , and the apparent volume of distribution during the terminal exponential phase, V_β , were calculated from the following equations:

$$V_c = \text{Dose}/C_0$$

$$V_\beta = \text{Dose}/(\text{AUC} \cdot \beta)$$

Hepatic uptake half-life was calculated from the following equations:

$$C_t/C_{tss} = 1 - e^{-kt}$$

$$t_{1/2} \text{ uptake} = 0.693/k$$

where C_t is the concentration in liver at time t and C_{tss} is the steady state concentration.

Values are expressed as mean \pm SE. Statistical comparison of values was accomplished with one-way ANOVA and Duncan's multiple range test.

RESULTS

General results

After an iv injection of a sublethal dose (35 $\mu\text{g/kg}$) of [^3H]MCYST-LR, the mice displayed normal behavior. Liver weight did not increase; and histologically, 1-60 min and 6 days post-exposure, livers were normal. Plasma levels of LDH, SDH, and AST were normal at 1 hr, transiently increased at 6 hr ($p < 0.01$, 10, 25, and 20-fold, respectively over control), and returned to normal by 12 hr. Levels of BUN and ALT were unaffected.

Clearance of toxin from plasma

The semilog plot of plasma concentration of toxin equivalents versus time is shown in Fig. 1. Results are presented as molar equivalents of toxin. The curve represents a biexponential decay with a maximum concentration of 428 pmol/ml. The half-lives of the α phase (distribution) and the β phase were 0.8 and 6.9 min, respectively. The AUC, estimated by the trapezoid rule, was 1036 pmol min/ml, and clearance from plasma was 0.9 ml/min. The apparent volume of the central compartment and V_β were 2 and 10 ml, respectively.

Concentration of toxin in tissues

The concentration of toxin molar equivalents per gram of tissue over time is shown in Fig 2. In liver, there was a rapid uptake of radiolabel, which reached a maximum accumulation of 521 ± 14 pmol/g ($71 \pm 3\%$ of dose) by 30 min. The half-life of uptake

was 6.8 min. In kidney, the maximum concentration was achieved at 3 min (90 ± 7 pmol/g, $4.6 \pm 0.6\%$ of dose) followed by a decline in concentration until 20 min. The amount of radiolabel in gut reached a maximum at 30-40 min. In lung and carcass, the maximum amounts were measured at 3 min, after which the concentration declined. Spleen and heart did not contain measurable amounts of radioactivity. The distribution of radiolabel to tissues with time, presented as percent of injected dose, is shown in Table 1. The overall recovery of radiolabel ranged from 74 to 101% of dose. The partition coefficients or distribution ratios (R_t , ratio of mean concentration of toxin equivalents in tissue to that in plasma) are given in Table 2. There was accumulation of radioactivity in liver, kidney, and intestine (ratio increased with time and was >1), but not in lung and carcass.

Excretion of [^3H]MCYST-LR in urine and feces.

Six days post-exposure to 35 $\mu\text{g/kg}$ [^3H]MCYST-LR, $23.7 \pm 1.7\%$ of the radiolabel was eliminated (Fig 3, Panel A); $9.2 \pm 1.0\%$ and $14.5 \pm 1.1\%$ via urine and feces, respectively. The percent of dose that appeared in feces or urine per collection interval is given in Fig. 3, panels B and C, respectively. The rate of elimination via feces was 0.9 and 0.5% per hr for 6 and 12 hr, and ca. 1% per day for the remaining 6 days. Within the first 12 hr, 74% of cumulative urinary excretion had occurred.

Metabolic fate of [³H]MCYST-LR.

Urine samples collected 6 and 12 hr after toxin exposure were analyzed for metabolites by C-18 HPLC. At 6 hr, $6 \pm 1\%$ of the injected radiolabel was found in urine; and $63 \pm 2\%$ ($n=7$) of that was parent toxin, rt 9.4 min (Fig. 4, panel B). The major portion of the remaining radiolabel ($30 \pm 4\%$) was associated with a peak of rt 4.5 min. There were also several minor peaks detected in some of the samples. Between 6 and 12 hr, $1.5 \pm 0.4\%$ of the radiolabel was excreted in urine. In the two samples that contained sufficient radioactivity to be analyzed, the profile was similar to that seen at 6 hr; 35% at rt 4.5 min and 63% as parent.

Feces collected 6 hr post injection contained $5 \pm 1\%$ of the injected radiolabel, $69 \pm 3\%$ of which was recovered for HPLC analysis. A typical radioactive profile for a 6-hr fecal sample is shown in Fig. 4, panel C. Parent toxin, rt 9.4 min, comprised $63 \pm 8\%$ ($n=6$) of the radioactivity with the residual in five other peaks (legend of Fig. 4). Between 6 and 12 hr, $2.9 \pm 0.3\%$ of the dose appeared in feces; $52 \pm 4\%$ was recovered for HPLC analysis, of which $76 \pm 8\%$ ($n=6$) was associated with parent toxin.

The total amount of liver-sequestered radiolabel did not change from 1 hr ($67 \pm 4\%$, $n=6$) to 6 days ($66 \pm 2\%$, $n=3$) post-exposure, while carcass-associated radiolabel, comprised of all tissues except liver, decreased from $15 \pm 2\%$ at 1 hr to trace amounts by 4 days. The subcellular distribution of hepatic

radiolabel also remained unchanged over 6 days; the 10,000 x g pellet, consisting of unbroken cells, mitochondria and plasma membrane, contained $13 \pm 1\%$; the 100,000 x g pellet, composed mainly of microsomes, residual plasma membrane, and mitochondria, contained $12 \pm 1\%$; and the cytosol contained $70 \pm 2\%$ of the hepatic radioactivity. Over the same time period, all cytosolic radiolabel eluted in the void volume of a DG10 desalting column, while free [^3H]MCYST-LR eluted as a lower molecular weight component (Fig. 5). After heat denaturation, pronase treatment and C-18 Sep Pak extraction, the Sep Pak-eluted radioactivity was separated into five radioactive, HPLC peaks of rt 4.9, 5.6, 6.6, 8.1, and 9.4 min, the latter being the rt of [^3H]MCYST-LR (Fig. 4, Panels D-F). The percent distribution of hepatic, cytosolic radiolabel with respect to time is presented in Tabel 3. The portion of radiolabel that remained bound to the C-18 Sep Pak resin plus that which remained insoluble decreased between 12 hr and 4 days, as did the 6.6 min HPLC peak. The 8.1-min fraction steadily increased while the 4.9- and 5.6-min peaks appeared at 6 hr and 12 hr, and disappeared after 2 and 6 days, respectively.

DISCUSSION

The kinetic parameters defined in this study indicate that plasma elimination did not reflect toxicity, as liver, the target organ, accumulated the toxin. Hepatic accumulation of [^3H]MCYST-LR has been observed by several groups (Pace *et al.*, 1990a,b; Robinson *et al.*, 1989; Brooks and Codd, 1987; Runnegar *et al.*, 1986; Falconer *et al.*, 1986); however, this is the first time that the long-term hepatic retention of radiolabel has been documented. Runnegar *et al.* (1986), who studied liver retention 24 hr post injection of various doses of [^{125}I]MCYST-YM, concluded that livers that were relatively normal by histological examination excreted almost all of the hepatic radioactivity, while those that exhibited more extensive damage retained the labeled toxin. It is not clear whether the discrepancy between their study and the data presented here is due to the difference in toxin variants or to the nature of the radiolabel attached to the compound. We found that the amount of radiolabel sequestered by liver peaked at 30 min and did not change thereafter over the 6-day study. The sequestered hepatic radiolabel appeared to be tightly bound to cytosolic protein, as evidenced by a) co-precipitation of radioactivity with protein after addition of TCA or organic solvents (data not shown), b) elution of radioactivity in the void volume of a DG10 desalting column (Fig. 5), and c) requirement for protease treatment prior to HPLC analysis. The large V_β , >300 ml/kg, is also indicative of extravascular tissue binding. Hepatic protein binding could explain the large liver-

to-plasma concentration ratio, as only unbound or free toxin could influence partitioning. Also, protein-bound toxin or metabolite would probably not follow typical xenobiotic elimination pathways, which could explain the long hepatic retention.

Fecal elimination, after the first 12 hr, was constant at ~1% per day; but the amount of hepatic radiolabel did not change over the course of the study. There was, however, a decrease in carcass (all tissues except liver) radioactivity over time, but it is not clear whether the radiolabel was eliminated directly or via bile. It is possible that toxin was taken up by gut ($8.6 \pm 0.7\%$ was found in gut at 1 hr) and subsequently excreted directly into the intestinal lumen and then eliminated in feces.

The major portion of urinary excretion occurred early and accounted for 9% of the dose. The limited urinary excretion is likely due to the rapid decline in plasma radiolabel. The half-life of the β phase of the plasma concentration curve and the hepatic uptake half-life were identical, ~7 min, indicating that liver was the major factor in the plasma elimination of [^3H]MCYST-LR. This is not surprising, as extravascular tissue binding is known to be a principle determinate of the apparent half-life of xenobiotics if V_d is >100 ml/kg. Drugs such as rifampicin that inhibit hepatic uptake of toxin (Pace et al., 1990a; Runnegar et al., 1981) increase its bioavailability and thus may increase the total urinary excretion.

Unlike the hepatic-cytosolic radiolabel, urine and fecal

radiolabel did not appear to be protein bound. Most of the radioactivity in both urine and feces was parent toxin (approximately 60%) and the metabolites that were detected did not appear to correlate with those seen in liver.

This study is the first to characterize over time the hepatic biotransformation of [³H]MCYST-LR. One hr post injection, two fractions other than parent were identified; the C-18 Sep Pak-bound\insoluble species and a radioactive HPLC peak of rt 6.6 min. Since the C-18 Sep Pak bound\insoluble radiolabel could not be further analyzed with the techniques employed, it is not clear if this fraction is composed of multiple chemical species. As this fraction and the 6.6-min peak decreased, between 12 hr and 4 days, three new radioactive peaks appeared, two transiently (rt = 4.9 and 5.6 min), and the third (rt of 8.1 min) increasingly. By 6 days the 8.1 min peak accounted for 60% of the cytosolic radiolabel. The parent peak, which also appeared to be protein bound, did not change substantially during the study. Pace et al. (1990a) studied livers perfused for 1 hr with lethal doses of [³H]MCYST-LR and described the insoluble/bound fraction, the 6.6 min rt peak, and parent compound. It, therefore, appears likely that the new HPLC peaks detected in this sublethal study represent the detoxification pathway for [³H]MCYST-LR and were not involved in manifestation of toxicity.

From the data presented in this study, it is clear that MCYST-LR forms a strong association with cytosolic protein.

Preliminary results from a subsequent study suggest that the association is covalent. Identification of the protein(s) involved may help in understanding the mechanism by which this cyclic peptide manifests its toxicity.

- ADAMS, W. H., STONE, J. P., SYLVESTER, B., STONER, R. D.,
SLATKIN, D. N., TEMPEL, N. R., and SIEGELMAN, H. W. (1988).
Pathophysiology of cyanoginosin-LR: *in vivo* and *in vitro* studies.
Toxicol. Appl. Pharmacol. **96**, 248-257.
- BEASLEY, V. R., COOK, W. O., DAHLEM, A. M., HOOSER, S. B.,
LOVELL, R. A., and VALENTINE, W. M. (1989). Algae intoxication in
livestock and waterfowl. *Vet. Clin. North Am. Food Anim. Pract.*
5, 345-361.
- BOTES, D. P., WESSELS, P. L., KRUGAR, H., RUNNEGAR, M. T. C.,
SANTIKARN, S., SMITH, R. J., BARNA, J. C. J., and WILLIAMS, D. H.
(1985). Structural studies on cyanoginosins-LR, -YR, -YA, and
-YM, peptide toxins from *Microcystis aeruginosa*. *Chem. Soc.*
Perkin Trans. 1, 2747-2748.
- BROOKS, W. P. and CODD, G. A. (1987). Distribution of *Microcystis*
aeruginosa peptide toxin and interactions with hepatic microsomes
in mice. *Pharmacol. Toxicol.* **60**, 187-191.
- FALCONER, I. R., BERESFORD, A. M. and RUNNEGAR, M. T. C. (1983).
Evidence of liver damage by toxin from a bloom of the blue-green
alga, *Microcystis aeruginosa*. *Med. J. Aust.* **1**, 511-514.
- FALCONER, I. R., BUCKLEY, T., and RUNNEGAR, M. T. C. (1986).
Biological half-life, organ distribution and excretion of ¹²⁵I-

labelled toxic peptide from the blue-green alga *Microcystis aeruginosa*. *Aust. J. Biol. Sci.* **39**, 17-21.

FOXALL, T. L. and SASNER, Jr., J. J. (1981). Effects of a hepatic toxin from the cyanophyte *Microcystis aeruginosa*. In *The Water Environment*, (W. W. Carmichael, Ed), pp. 365-387. Plenum Press, New York.

GALEY, F. D., BEASLEY, V. R., CARMICHAEL, W. W., KLEPPE, G., HOOSER, S. B., and HASCHEK, W. M. (1987). Blue-green algae (*Microcystis aeruginosa*) hepatotoxicosis in dairy cows. *Am. J. Vet. Res.* **48**, 1415-1420.

HOOSER, S. B., BEASLEY, V. R., LOVELL, R. A., CARMICHAEL, W. W., and HASCHEK, W. M. (1989). Toxicity of microcystin LR, a cyclic heptapeptide hepatotoxin from *Microcystis aeruginosa*, to rats and mice. *Vet. Pathol.* **26**, 246-252.

JACKSON, A. R., McINNES, A., FALCONER, I. R., and RUNNEGAR, M. T. C. (1984). Clinical and pathological changes in sheep experimentally poisoned by the blue-green alga *Microcystis aeruginosa*. *Vet. Pathol.* **21**, 102-113.

JUNGERMANN, K. and KATZ, N. (1989). Functional specialization of different hepatocyte populations. *Phys. Rev.* **69**, 708-764.

KONST, H., MCKERCHER, P. D., GORHAM, P. R., ROBERTSON, A., and HOWELL, J. (1965). Symptoms and pathology produced by toxic *Microcystis aeruginosa* NRC-1 in laboratory and domestic animals. *Can. J. Comp. Med. Vet. Sci.* **29**, 221-228.

MATSUO, H. and NARITA, K. (1975). Improved tritium-labeling for quantitative C-terminal analysis. In *Protein Sequence Determination, a Source Book of Methods and Techniques*, (S. B. Needleman, Ed.), pp. 104-113. Springer-Verlag, New York.

PACE, J. G., RIVERA, E., ROBINSON, N. A., LYNCH T., MIURA, G. A., MATSON, C. F., and LAWRENCE, W. B. (1990a). Toxicokinetics and treatment of microcystin-LR in perfused livers. *Toxicon* (in press, abstract)

PACE, J. G., ROBINSON, N. A., MIURA, G. A., LYNCH T. G., and TEMPLETON, C. B. (1990b). Pharmacokinetics, metabolism and distribution of microcystin in the rat. *The Toxicologist* **10**, 219. (Abstract 873)

PELKONEN, O. (1979). Prenatal and neonatal development of drug and carcinogen metabolism. In *The Induction of Drug Metabolism*, (R. W. Estabrook and E. Lindenlaub, Eds.), pp. 507-516. F. K. Schattauer Verlag, New York.

RINEHART, K. L., HARADA, K., NAMIKOSHI, M., CHEN, C., HARVIS, C.

A., MUNRO, M. H. G., BLUNT, J. W., MULLIGAN, P. E., BEASLEY, V. R., DAHLEM, A. M., and CARMICHAEL, W. W. (1988). Nodularin, microcystin, and the configuration of Adda. *J. Am. Chem. Soc.* **110**, 8557-8558.

ROBINSON, N. A., MIURA, G. A., MATSON, C. F., DINTERMAN, R. E., and PACE, J. G. (1989). Characterization of chemically tritiated microcystin-LR and its distribution in mice. *Toxicon* **27**, 1035-1042.

RUNNEGAR, M. T. C., FALCONER, I. R., BUCKLEY, T., and JACKSON, A. R. B. (1986). Lethal potency and tissue distribution of ¹²⁵I-labelled toxic peptides from the blue-green alga *Microcystis aeruginosa*. *Toxicon* **24**, 506-509.

RUNNEGAR, M. T., FALCONER, I. R., and SILVER, J. (1981). Deformation of isolated rat hepatocytes by a peptide hepatotoxin from the blue-green alga *Microcystis aeruginosa*. *Naunyn-Schmiedeberg's Arch. Pharmacol.* **317**, 268-272.

SOLL, M. D. and WILLIAMS, M. C. (1985). Mortality of a white rhinoceros (*Ceratotherium simum*) suspected to be associated with the blue-green alga *Microcystis aeruginosa*. *J. South African Veterinary Association* **56**, 49-51.

STONER, R. D., ADAMS, W. H., SLATKIN, D. N., and SIEGELMAN, H. W.

(1989). The effects of single L-amino acid substitutions on the lethal potencies of the microcystins. *Toxicon* 27, 825-828.

THEISS, W. C., CARMICHAEL, W. W., WYMAN, J., and BRUNER, R.

(1988). Blood pressure and hepatocellular effects of the cyclic heptapeptide toxin produced by the freshwater cyanobacterium (blue-green alga) *Microcystis aeruginosa* strain PCC-7820. *Toxicon* 26, 603-613.

The views of the authors do not purport to reflect the positions of the Department of the Army or the Department of Defense (para. 4-3, AR 360-5). In conducting research described in this report, the investigators adhered to the "Guide for the Care and Use of Laboratory Animals," as promulgated by the Committee on the Care and Use of Laboratory Animals of the Institute of Laboratory Animal Resources, National Research Council. The facilities are fully accredited by the American Association for Accreditation of Laboratory Animal Care.

The authors thank Everett Lucas, Thomas Lynch, and Karen Bostian for excellent technical assistance; Dr. David Franz and Mr. Richard Dinterman for assistance in animal handling.

Portions of this data have been published in abstract form FASEB J (in press).

TABLE 1. DISTRIBUTION OF RADIOLABEL OVER TIME^a

TIME (min)	% DOSE			
	LIVER	KIDNEY	INTESTINE	CARCASS
1	23 ± 5	2.0 ± 0.2	5.2 ± 0.9	30 ± 3
3	56 ± 6	4.6 ± 0.6	4.6 ± 0.5	27 ± 4
6	55 ± 2	2.1 ± 0.3	7.1 ± 0.5	20 ± 5
10	50 ± 1	1.1 ± 0.1	4.7 ± 0.5	16 ± 4
15	60 ± 5	1.2 ± 0.1	5.8 ± 0.7	17 ± 4
20	66 ± 5	0.8 ± 0.2	6.1 ± 1.3	11 ± 3
30	71 ± 3	0.7 ± 0.1	6.8 ± 0.7	3 ± 1
40	69 ± 5	0.9 ± 0.1	10.5 ± 1.0	6 ± 2
60	67 ± 4	0.8 ± 0.1	8.6 ± 0.7	6 ± 2
				0

^aValues are mean ± SE, n=6.

TABLE 2. DISTRIBUTION RATIO (R_i)^a

TIME (min)	LIVER	KIDNEY	INTESTINE	LUNG	CARCASS
1	0.85	0.20	0.07	0.17	0.07
3	5.68	1.33	0.23	0.33	0.19
6	12.88	1.34	0.81	0.33	0.25
10	17.83	1.05	0.76		0.35
15	36.60	1.86	1.63		0.63
20	64.49	1.75	3.10		0.55
30	206.17	4.13	11.20		0.56
40	538.52	18.34	46.50		3.20

^aValues are the ratio of the mean tissue concentration to the mean plasma concentration.

TABLE 3. DISTRIBUTION OF HEPATIC CYTOSOLIC RADIOLABEL (% OF TOTAL)^a

TIME	SEP PAK ^b	HPLC RETENTION TIME (MIN)			
		4.9	5.6	6.6	8.1
1 H	35 ± 2	0	0	43 ± 3	0
6 H	41 ± 5	0	4 ± 1	41 ± 3	0
12 H	40 ± 3	T ^d	7 ± 1	34 ± 3	T
1 D	30 ± 4	5 ± 0	12 ± 1	33 ± 3	7 ± 1
2 D	19 ± 3	3 ± 2	9 ± 2	20 ± 1	25 ± 1
4 D	10 ± 2	0	4 ± 1	14 ± 2	45 ± 2
6 D	8 ± 1	0	T	5 ± 0	60 ± 2
CONTROL ^c	9 ± 1	0	0	0	0
					90 ± 1

^aValues are mean ± SE, n=3.

^b% of hepatic cytosolic radiolabel which pelleted after pronase digestion + that which remained bound to the Sep Pak C-18 resin.

^cRetention time of [³H]MCYST-LR.

^dTrace amount detected.

^eControl liver cytosol was prepared, heat denatured and spiked with 30,000 dpm of [³H]MCYST-LR. The samples were then processed as described in Methods.

FIGURE LEGENDS

Fig. 1. Semilog plot of plasma concentration of toxin equivalents versus time. The open circles represent the mean \pm SE for six animals per time point. The solid line is the theoretical curve defined by the inset equation.

Fig. 2. Semilog plot of tissue concentration of toxin equivalents versus time. The values presented are the mean \pm SE for six animals per time point. The symbols represent the following tissues: (○) liver, (●) kidney, (▲) carcass, (■) lung, and (△) gut.

Fig. 3. Appearance of radioactivity in urine and feces. Panel A is the cumulative urinary and fecal appearance of radioactivity. Panel B is the percent of injected dose that appeared in feces per collection period. Panel C is the percent of dose that appeared in urine per collection period. Values are mean \pm SE, $n = 9-13$

Fig. 4. C-18 HPLC profile of radiolabel in urine, feces, and hepatic cytosol. Panel A: [3 H]MCYST-LR in control fecal extract. Control urines or control, heat-denatured hepatic cytosol that were spiked with [3 H]MCYST-LR yielded identical results. Panel B: representative 6-hr urine, analysis was performed without prior treatment. Panel C: representative 6 hr fecal extract

prepared as described in Methods. The fecal extracts were darkly colored, which appeared to affect counting efficiency of the Radiomatic Flow I β counter. The following peaks at the indicated rt were detected (mean % of total radioactivity \pm SE) in n out of six samples: 4.0 min, 13% (n=2); 4.6 min, $9 \pm 2\%$ (n=4); 5.3 min, 6.5% (n=2); 6.3 min, $20 \pm 4\%$ (n=5); 8.4 min, $11 \pm 3\%$ (n=4); and [^3H]MCYST-LR, 9.3 min, $63 \pm 8\%$ (n=6). Panels D-F: representative hepatic cytosol profiles 6 hr, 1 day and 6 days post injection, respectively. Cytosols were prepared for analysis as described in Methods. The [^3H]MCYST-LR peak is indicated by <- M.

Fig. 5. Econo-Pac 10DG desalting column profile of radiolabel. Samples (0.8 ml) of liver cytosol were chromatographed on a 10-ml Bio-Gel P-6 column and 1-ml fractions were collected. The solid line is a representative elution pattern from cytosol 2 days post injection. All the time points, 1 hr through 6 days, were identical. The dashed line is the elution profile of [^3H]MCYST-LR. V_0 indicates the void fraction of the column measured with blue dextrin.

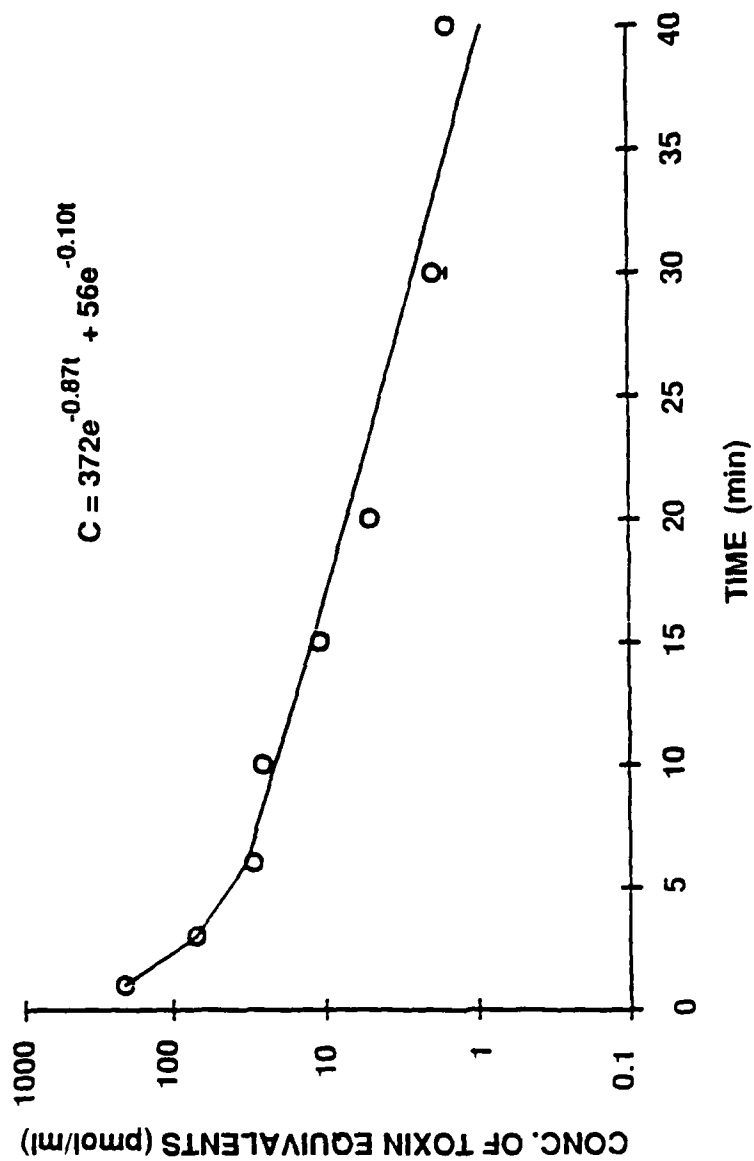


figure 1

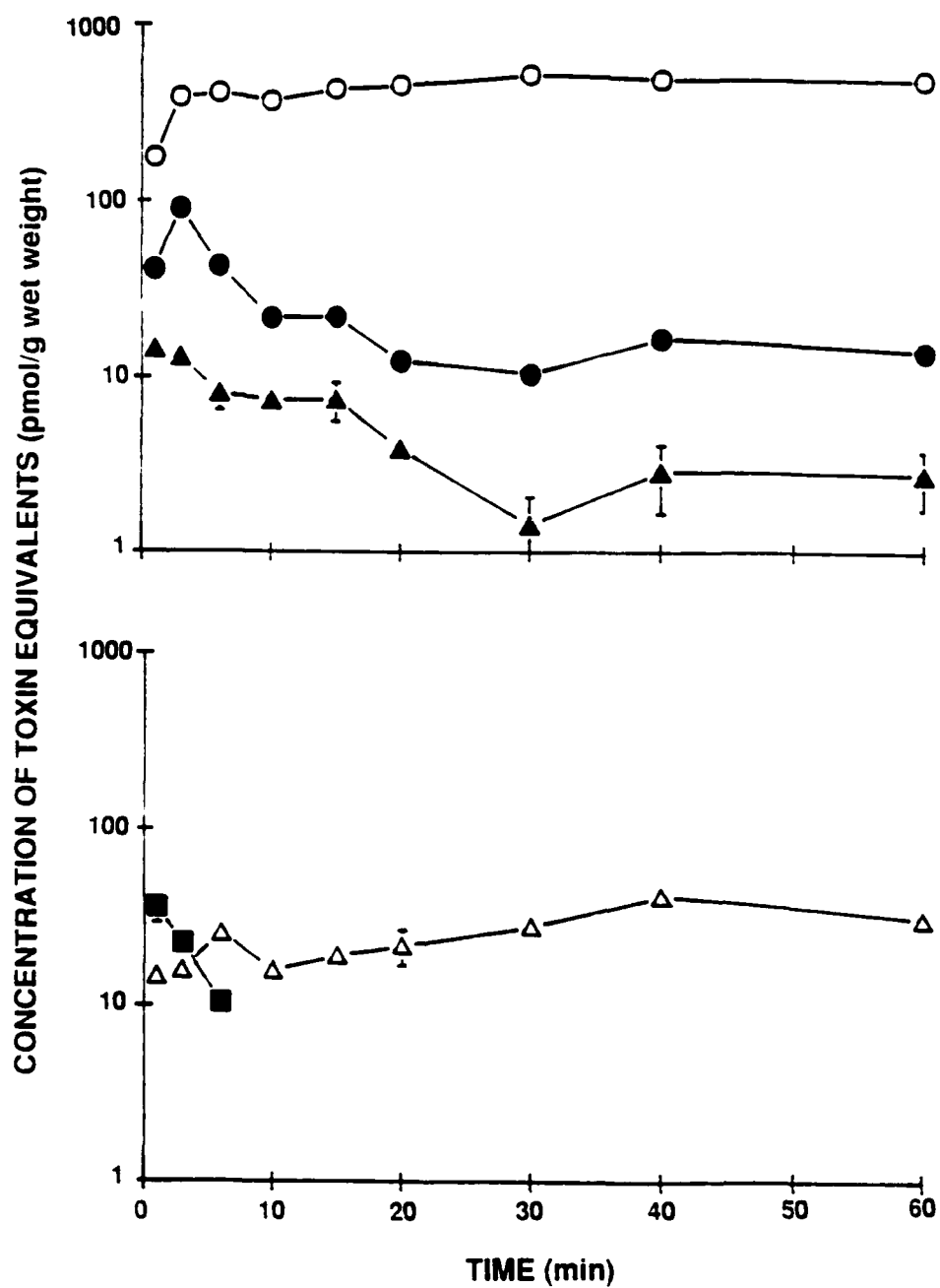
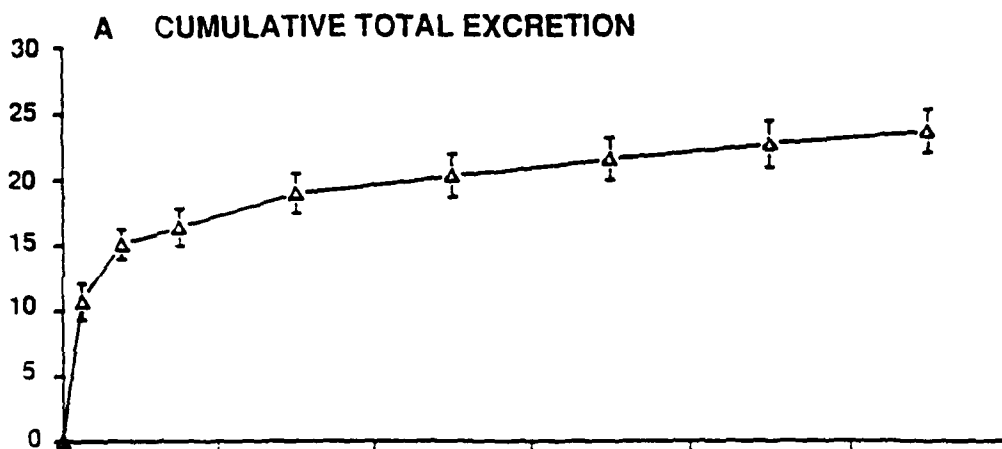
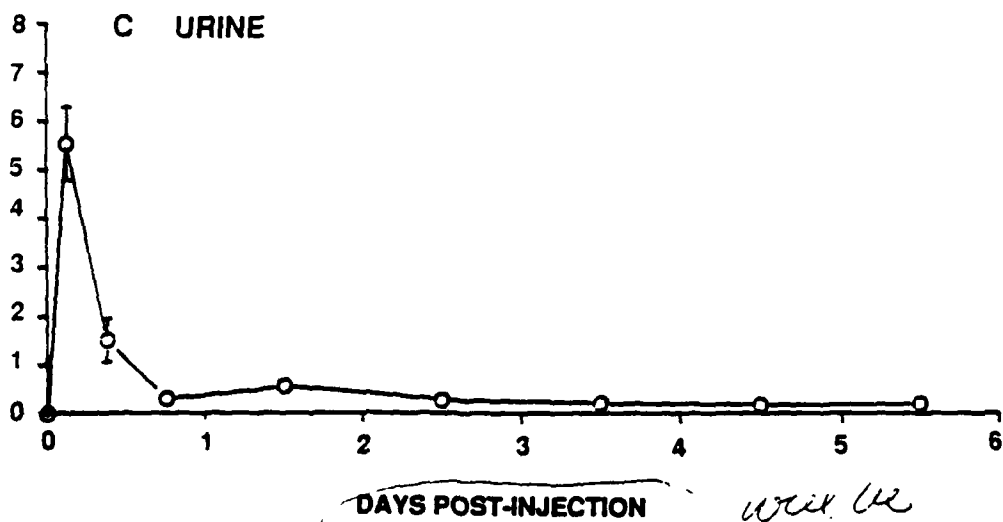
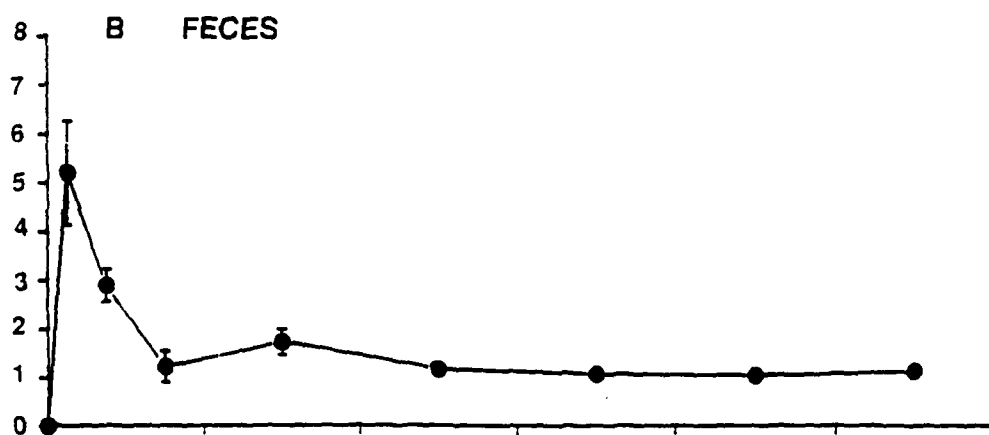


fig 2

will be integrated



%DOSE INJECTED



will be integrated

Fig 3

RELATIVE COUNTS

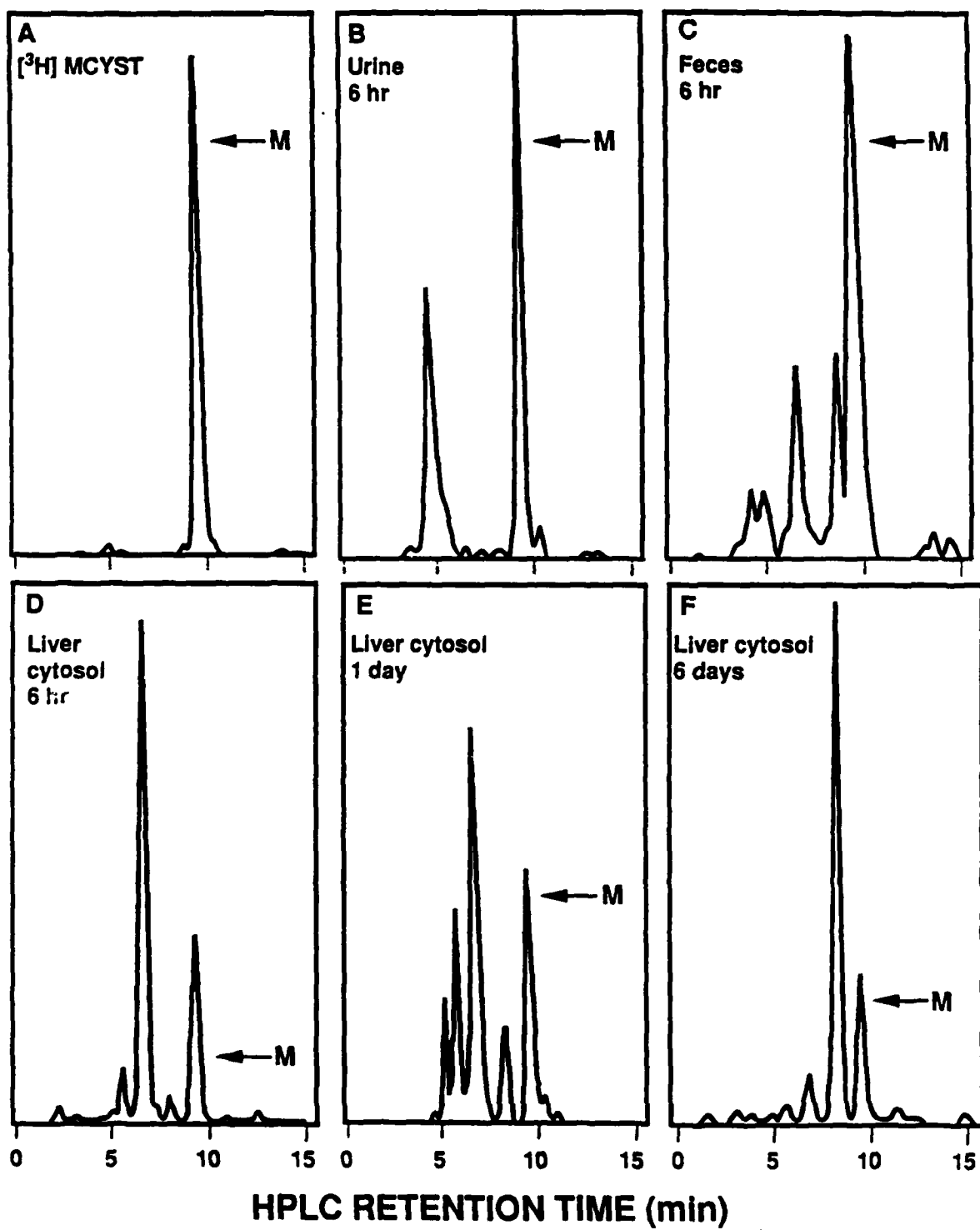


Fig 4

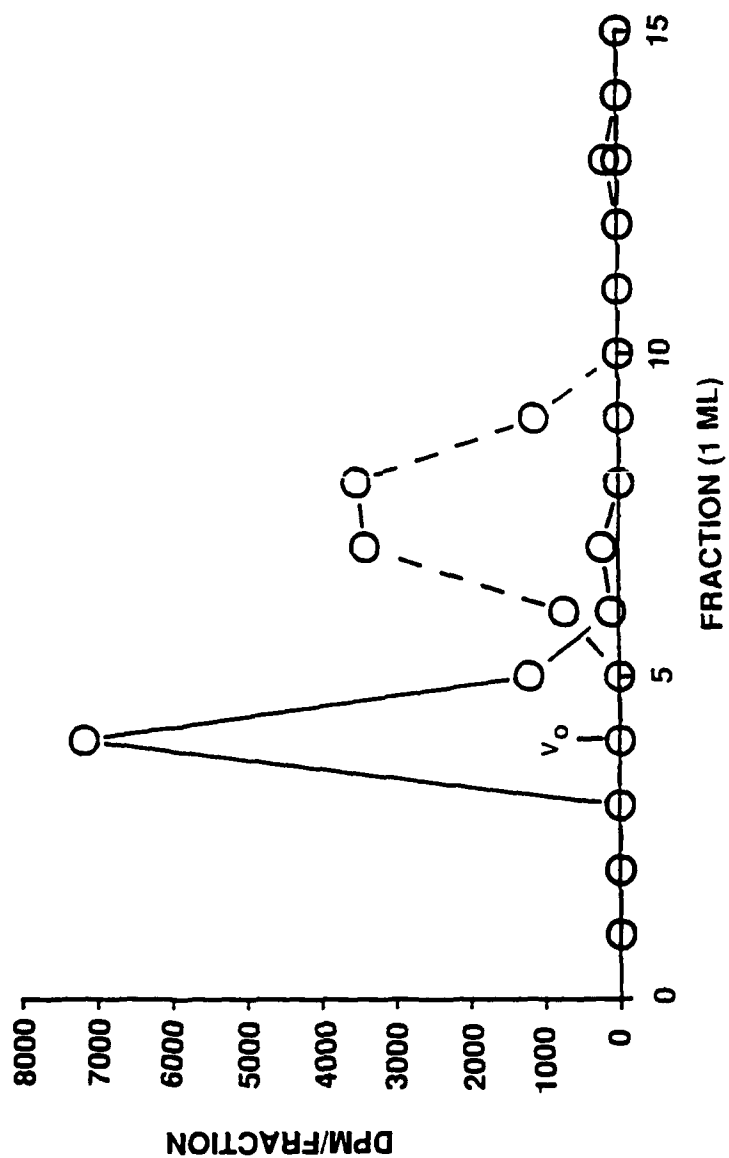


figure 5